2013 European Control Conference (ECC)
July 17-19, 2013, Zürich, Switzerland.

Temperature Control of the FTU Liquid Lithium Limiter

L. Boncagni, D. Carnevale, A. Cristaldi, S. De Maio,
G. Mazzitelli, M. Sassano, V. Vitale, R. Vitelli, L. Zaccarian

***Abstract*— Several experiments on Tokamak devices have shown serious difficulties in the development of appropriate technical solutions concerning the structure and material composition of the plasma-facing elements. For instance the first wall ($i.e.$ the innermost surface of the Tokamak vacuum chamber), the limiters and the divertors are a main concern due to the neutron flux and the thermal loads. A possible solution is to abandon solid plasma facing materials, using liquid metals instead. In the FTU (Frascati Tokamak Upgrade) an experimental Liquid Lithium Limiter (LLL) has been installed and tested, by empirically tuning the plasma position in order to prevent the modules of the limiter from reaching critical temperatures. In this paper we propose two alternative nonlinear control strategies for the temperature regulation of the surfaces of the LLL modules. The paper is concluded with numerical simulations that validate the performances of the proposed approaches.**

I. Introduction

Avoiding thermal and neutronic damages to the plasma-facing components of a Tokamak machine – such as the first wall, the divertors and the limiter – is a crucial issue in current fusion experimental devices, hence in future fusion power plants. Several approaches have been proposed in recent years to tackle the problem. Among these, a possible methodology is to abandon solid materials, using instead liquid metals with low atomic mass and activation, such as liquid lithium.

To this end, a Liquid Lithium Limiter (LLL) has been deployed in FTU. Due to its small size, the FTU-LLL cannot act as the machine only limiter and it needs to be operated in combination with the main limiter. Nonetheless, the approach has already shown promising results [1]. The main issue associated with this experimental limiter is to keep the temperatures of the three modules that create the Liquid Lithium Limiter under a certain threshold (approximately $470^{\circ}C$) in order to avoid damages to the structure, on one hand, and to limit the amount of lithium in the plasma itself, on the other hand. Indeed at higher temperatures the consequent lithium evaporation increases the amount of impurities affecting the plasma. Temperature control of the LLL is currently achieved empirically by means of a feed-forward scheme which modifies the *pre-programmed* plasma position (namely the plasma position reference). Indeed the temperature of the LLL is significantly affected by its distance from the (hot) plasma. The problem of defining a feedback strategy to adjust the plasma position to steer the temperatures towards desired values is studied in this paper.

The feedback controller designed here should also fit in the current architecture of the FTU Plasma Control System (PCS), without modifying its structure. This can be obtained by following a pattern already successfully applied in previous works carried out on the PCS, such as the upgrade with an antiwindup approach to the AL/F current feedback [2], the RF optimization algorithm for the LH antenna [3], and a dynamic allocation algorithm to control the elongation of the plasma [4]. In all these schemes, the control task is accomplished by injecting suitable continuous modifications to the reference signals of the existing controllers, thus performing the additional task in a secure way. Since an upgrade project has been carried out on the PCS, which is being revamped and ported to a new MARTe-based architecture [5], [6], the task may be easily completed by developing a GAM, $i.e.$ a "pluggable module" for the FTU real-time controller.

The main contributions of this paper consist in the description of the control problem by a suitable mathematical model and the development of two alternative approaches to tackle the problem of controlling the temperatures of the modules of the FTU-LLL. The first approach hinges upon a Jacobian matrix inversion and permits the assignment of any desired behavior to the modules temperatures via the definition of their second time derivatives. The second approach is inspired by a gradient-like algorithm and operates towards the minimization of the heat absorbed by the modules, avoiding computational and numerical problems intrinsically generated by the matrix inversion of the first approach.

The rest of the paper is organized as follows: after a brief introduction of the Liquid Lithium Limiter (LLL), in Section II we illustrate the approximate model employed to describe the evolution over time of the temperatures of the modules. This simplified model is then exploited for the feedback control design in Section III. Finally, numerical simulations that corroborate the effectiveness of the proposed technique are reported in Section IV.

II. LLL Temperature model

The Liquid Lithium Limiter deployed at FTU consists of three distinct modules, each one of them devised using the CPS (Capillary Porous System) configuration, see [1] for a more detailed discussion. The temperature of the modules is measured via three infrared cameras placed at the top of the vacuum chamber, each one pointing at a single module. The derivation of an approximate model for the temperatures of the LLL modules is described in this section.

A. Basic definitions and assumptions

Two different sets of parameters are involved in the definition of such a model, namely the plasma magnetic parameters

$$p = (\Delta\Psi_R, \Delta\Psi_Z, e) \tag{1}$$

L. Boncagni, G. Mazzitelli and V. Vitale are with EURATOM - ENEA Fusion Association, Frascati Research Centre, Division of Fusion Physics, Rome, Frascati, ITALY (luca.boncagni@enea.it)

D. Carnevale, A. Cristaldi, S. De Maio, M. Sassano, R. Vitelli are with the Dipartimento di Ingegneria Civile e Ingegneria Informatica, University of Rome Tor Vergata, Rome, ITALY (mario.sassano@uniroma2.it)

L. Zaccarian is with CNRS, LAAS, 7 avenue du colonel Roche, F-31400 Toulouse, France and Univ de Toulouse, LAAS, F-31400 Toulouse, France. zaccarian@laas.fr. L. Zaccarian is also with the University of Trento, Italy.

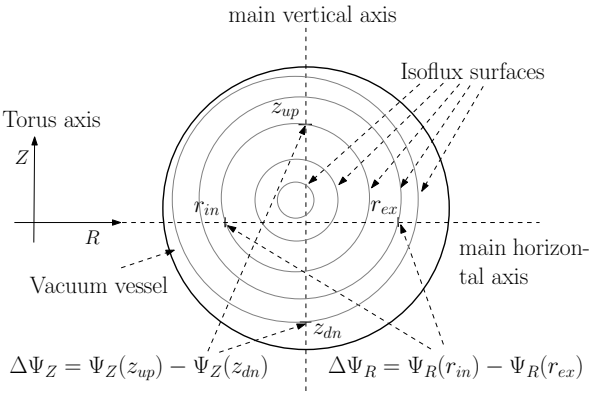

Fig. 1. Definition of $\Delta\Psi_R$ and $\Delta\Psi_Z$.

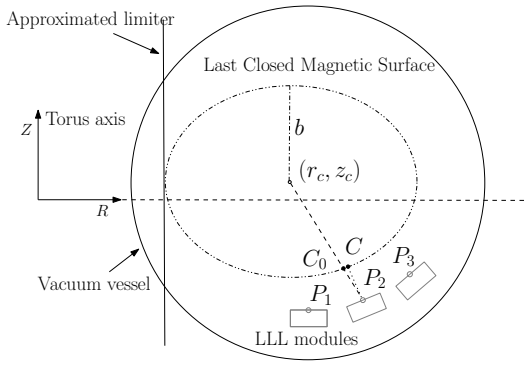

Fig. 2. Toroidal section of the vacuum chamber (solid circle) together with the distance between P_2 and the Last Closed Magnetic Surface (dash-dotted) $\overline{P_2C}$ and its approximation $\overline{P_2C_0} \triangleq d_2$.

and the plasma configuration parameters

$$\mu = (r_c, z_c, b)\,. \tag{2}$$

Parameters in (1) describe the magnetic properties and the elongation of the plasma. In particular, let $\Psi_R(r)$ denote the value of the (axial-symmetric) flux along the main horizontal axis R of the torus section, evaluated at r. Similarly, let $\Psi_Z(z)$ denote the value of the flux along the main vertical axis Z of the section, evaluated at z. Then $\Delta\Psi_R = \Psi_R(r_{in}) - \Psi_R(r_{ex})$ represents the difference between the magnetic flux evaluated at the internal r_{in} and the external r_{ex} pre-programmed rays along the main horizontal axis of the torus cross section (see Figure 1). Since r_{in} is always selected as the coordinate of the inner plasma limiter, we will enforce this constraint here to simplify our equations (the general case simply involves an extra bias term). Similarly, $\Delta\Psi_Z = \Psi_Z(z_{up}) - \Psi_Z(z_{dn})$ is the difference between the flux evaluated at the upper z_{up} and the lower z_{dn} pre-programmed rays along the main vertical axis. On the other hand, referring to Figure 2 parameters μ in (2) summarize the position of the plasma center inside the vacuum chamber (r_c and z_c denote the coordinates of the center of the plasma) and the length b of the vertical semi-axis[1] of the ellipse describing the Last Closed Magnetic Surface.

Finally, we suppose that the Last Closed Magnetic Surface is *limited*, on the internal boundary of the torus, by a vertical line, see Figure 2. This assumption, which greatly simplifies the derivation of the model, may be removed considering more complex shapes of the plasma limiter, at the price of complicating the function ϕ in (4) and q_0 in (6). A direct consequence of the previous assumption is that the length of the horizontal semi-axis a of the ellipse is obtained as $a = r_c - r_{in}$, where the internal radius r_{in} coincides with the distance of the vertical limiter from the origin of the reference frame, which is fixed at the center of the torus, as shown in Figure 2.

B. Model

In order to derive the model, the two sets of parameters (1) and (2) are combined together, as detailed in the following, by determining firstly the relation between them and then between μ and the heat transferred to the modules. We now discuss the relation between the two sets of parameters p and μ defined in (1) and (2), respectively, which is given in terms of an implicit function. More precisely, we seek for a mapping $\phi : \mathbb{R}^3 \times \mathbb{R}^3 \to \mathbb{R}^3$ such that $\phi(p, \mu) = 0$. Towards this end, we suppose that the magnetic flux generated along the R-axis[2] can be described by the Gaussian function

$$\Psi_R(r) = c_R + A_R e^{-\dfrac{(r - r_c)^2}{\gamma_R}}, \tag{3}$$

where the parameters c_R, $A_R > 0$ and $\gamma_R > 0$ have to be appropriately selected and may be different for different experiments (the constant c_R will not play any role in the computation of $\Delta\Psi_R$). To test the validity of this assumption, an example is shown in Figure 3 that represents the flux Ψ_R at different time instants during the experiment #36065 together with the approximation as in (3) (dashed line), which is obtained by letting $c_R = -0.1$, $A_R = 0.65$ and $\gamma_R = 0.045$. Since the scheme proposed in the following section adjusts the position of the plasma inside the vessel via (relatively small) deviations from a desired configuration, the approximation should be more accurate in the regions closer to the pre-programmed rays, namely around $r_{in} \approx 0.645m$ and $r_{ex} \approx 1.225m$. Then, recalling the definition of $\Delta\Psi_R$, equation (3) yields[3]

$$\Delta\Psi_R = A_R \left(e^{-\frac{(r_{in} - r_c)^2}{\gamma_R}} - e^{-\frac{(r_{ex} - r_c)^2}{\gamma_R}} \right).$$

Moreover, by definition of elongation $e = b/a$ and by the previous simplifying assumption on the structure of the limiters, we have $e = b/(r_c - r_i)$. Therefore, the mapping ϕ may be written as

$$\phi(p, \mu) = \begin{bmatrix} \Delta\Psi_R - A_R \left(e^{-\frac{(r_{in} - r_c)^2}{\gamma_R}} - e^{-\frac{(r_{ex} - r_c)^2}{\gamma_R}} \right) \\ \Delta\Psi_Z - A_Z \left(e^{-\frac{(z_{up} - z_c)^2}{\gamma_Z}} - e^{-\frac{(z_{dn} - z_c)^2}{\gamma_Z}} \right) \\ e - \frac{b}{rc - r_{in}} \end{bmatrix}. \tag{4}$$

The Implicit Function theorem [8] guarantees the existence and uniqueness of a continuously differentiable mapping $g : \mathbb{R}^3 \to \mathbb{R}^3$ such that $\mu = g(p)$ and $\phi(p, g(p)) = 0$ as long

[1]The reason for not considering the length of the horizontal semi-axis a as a free parameter will become clear shortly.

[2]Identical considerations apply to the magnetic flux along the Z-axis.

[3]Note that, by definition of the Gaussian function in (3), $\Psi_R(r_{LCMS}) = \Psi_R(r_{in})$.

as the Jacobian matrix of ϕ with respect to μ is non-singular, which is a condition that has been checked numerically for the parameter values characterizing the FTU experiment. While we know that g exists, its explicit expression may be very difficult if not impossible to compute. However its Jacobian $\frac{\partial g(p)}{\partial p}$ can be explicitly computed and its knowledge will be used in the control schemes that we propose in the next section.

The second part of our model comprises the relation between the plasma configuration parameters μ and the heat transferred to the modules. To begin with, the approximate[4] Euclidean distance d_i between the center of the i-th LLL module surface and the plasma boundary (LCMS) can be obtained by computing the intersection C_0 between the segment from $P_i = (x_{p_i}, y_{p_i})$ to (r_c, z_c) (dashed in Figure 2) and the dash-dotted ellipse in Figure 2 representing the plasma boundary centered at (r_c, z_c), *i.e.*

$$\frac{(r - r_c)^2}{(r_c - r_{in})^2} + \frac{(z - z_c)^2}{b^2} = 1.$$

Then we can write d_i, $i = 1, 2, 3$, as an explicit function of the plasma configuration parameters corresponding to

$$d_i(\mu, P_i) = \sqrt{(x_{p_i} - x_{C_0})^2 + (y_{p_i} - y_{C_0})^2}\,, \qquad (5)$$

where (x_{C_0}, y_{C_0}) denote the coordinates of the intersection.

Moreover, the density function of the thermal power radiated by the plasma surface is given by [9]:

$$q_0(\mu, I_p, V_{loop}) = 0.9 \frac{I_p V_{loop}}{4\pi^2 r_c \sqrt{(r_c - r_i)b}}, \qquad (6)$$

where I_p corresponds to the current induced by the plasma, and V_{loop} corresponds to the voltage induced by the plasma. I_p and V_{loop} are measured by the real-time control system during the experimental pulse. Equation (6) may be interpreted as the power $I_p V_{loop}$ over the total surface of the plasma, which possesses a toroidal geometry. The surface can be obtained by rotation of the perimeter of a single poloidal section (as in Figure 2 and approximated by $2\pi\sqrt{(r_c - r_i)b}$) around the axis of the torus, namely multiplying the perimeter by $2\pi r_c$. Then, based on equations (5) and (6), the heat transferred within the vacuum vessel to the i-th LLL module is given by [9]:

$$Q_i(\mu, I_p, V_{loop}) = q_0(\mu, I_p, V_{loop}) e^{-\frac{d_i(\mu, P_i)}{\lambda_E}}, \qquad (7)$$

where $\lambda_E > 0$ is a factor characterizing the power decay rate according to the distance from the source.

Finally, combining the two previous steps, the evolution of the three LLL modules temperature $T \in \mathbb{R}^3$ is approximated by the first-order ordinary differential equation

$$\dot{T} = \rho \tilde{Q}(p, I_p, V_{loop}) - \Lambda(T - T_{\rm eq}), \qquad (8)$$

where $\tilde{Q}(p, I_p, V_{loop}) = Q(g(p), I_p, V_{loop})$, $\rho > 0$ is related to the specific heat and module density, $\Lambda = \mathrm{diag}\{\lambda_1, \lambda_2, \lambda_3\} > 0$ comprises the coefficients of the modules thermal conductivities, $T_{\rm eq}$ represents the temperature that the modules would reach in the absence of the heat radiating from the plasma. It is clear from (8) that the only way to dissipate heat is by means of the modules thermal conductivity Λ.

[4]The exact distance between the center of the LLL module, i.e. the length of the segment perpendicular to the plasma boundary that starts at P_1 and ends at the plasma boundary (see $\overline{P_1 C}$ in Figure 2), cannot be calculated explicitly since it would require to solve a fourth-order polynomial and a nontrivial trigonometric equation.

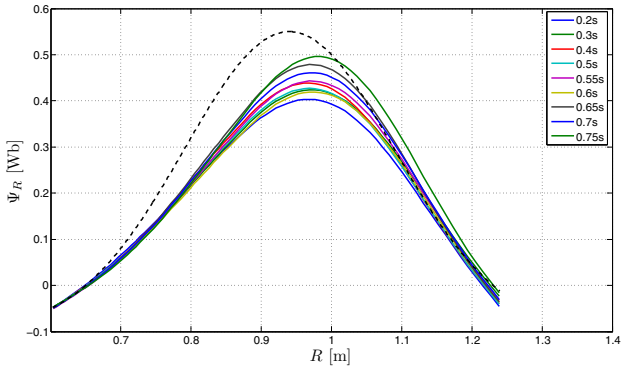

Fig. 3. Approximation of the magnetic flux Ψ_R obtained as in (3) with $c_R = -0.1$, $A_R = 0.65$ and $\gamma_R = 0.045$ (dashed line) and its measurement at various sampling times (solid lines) during an experiment (shot #36065) .

III. Control Scheme

In this section we discuss the proposed control schemes. Towards this end, let $p_0 = (\Delta\Psi_R^0, \Delta\Psi_Z^0, e^0) \in \mathbb{R}^3$ be the *pre-programmed* plasma magnetic parameters. Then, the problem to be solved is formally introduced in the following definition.

Problem 1: Given a triple $T_{\rm ref}$ of desired temperatures for the three LLL modules, choose a continuous perturbation p_δ of reference plasma magnetic parameters such that using $p(t) = p_0 + p_\delta(t)$ the temperatures $T(t)$ given by (5)-(8) remain bounded for all $t \geq 0$ and tend to $T_{\rm ref}$ as t goes to infinity. □

It appears evident that p_δ describes the variations of $(\Delta\Psi_R, \Delta\Psi_Z, e)$ with respect to the *pre-programmed* value p_0, namely a deviation from a nominal behavior. This type of structure is fundamental to allow for the integration of the proposed controller within the current plasma control system (see also Figure 4). The following assumption is instrumental for the construction of a solution to Problem 1, which ensures exponential convergence to the desired reference value $T_{\rm ref}$.

Assumption 1: Let I_p and V_{loop} be constant[5] in (6). Furthermore, assume that there exists $\epsilon > 0$ such that

$$\frac{\partial \tilde{Q}}{\partial p} \left(\frac{\partial \tilde{Q}}{\partial p} \right)^\top > \epsilon I, \qquad (9)$$

for all $p \in \mathbb{R}^3$, where $I \in \mathbb{R}^{3\times 3}$ is the identity matrix. □

To streamline the presentation of the main result of this section, which provides a solution to Problem 1, define $x_1 = T - T_{\rm ref} \in \mathbb{R}^3$ and $x_2 = \dot{T} \in \mathbb{R}^3$. Note that only x_1 is directly measured. Based on the model (8), the variables

[5]I_p and V_{loop} are indeed constant in the flat-top phase of the experimental pulse, i.e. during the main part of the experiment.

$x_1(t)$ and $x_2(t)$ evolve according to ordinary differential equations described by

$$\dot{x}_1 = x_2, \tag{10a}$$

$$\dot{x}_2 = \rho \frac{\partial \tilde{Q}}{\partial p}(p)\dot{p}_\delta - \Lambda x_2. \tag{10b}$$

Moreover, define the matrices

$$F = \begin{bmatrix} 0 & I \\ 0 & -\Lambda \end{bmatrix} \tag{11}$$

and $C = [I,\, 0]$. A suitable choice of the dynamics of the variation p_δ, *i.e.* $\dot{p}_\delta$, allows us to determine a solution to Problem 1, as detailed in the following result. The solution corresponds to the block diagram of Figure 4.

Theorem 1: Consider system (10) and suppose that Assumption 1 holds. Select

$$\dot{\hat{x}} = F\hat{x} + \begin{bmatrix} 0 \\ I \end{bmatrix} \rho \frac{\partial \tilde{Q}}{\partial p}(p)\dot{p}_\delta + L(x_1 - \hat{x}_1), \tag{12a}$$

$$\dot{p}_\delta = \frac{1}{\rho} k(p, \mu, I_p, V_{loop}) \left(-\alpha_1 x_1 + (\Lambda - \alpha_2 I)\hat{x}_2\right), \tag{12b}$$

with α_1 and α_2 any two positive constants, where $L \in \mathbb{R}^{6\times 3}$ is such that $F - LC$ has all the eigenvalues with strictly negative real part and

$$k(p, \mu, I_p, V_{loop}) = -\frac{\partial \phi}{\partial \mu}(p, \mu) \left(\frac{\partial Q}{\partial \mu}(\mu, I_p, V_{loop})\right)^{-1}. \tag{13}$$

Let $\eta = x - \hat{x}$. Then, the zero equilibrium $(x_1, x_2, \eta) = (0, 0, 0)$ of the closed-loop (10)-(12) is globally exponentially stable, hence (12) provides a solution to Problem 1. □

Remark 1: Since in practice the magnetic parameters p are upper and lower bounded, an equivalent characterization of Assumption 1 may be given, allowing for a more intuitive interpretation of the requirement. More precisely, we may alternatively suppose that

$$\det\left(\frac{\partial \tilde{Q}}{\partial p}(p)\right) \neq 0, \tag{14}$$

for all $p \in \mathcal{W}$, where $\mathcal{W}$ is a suitable compact set dependent on the experimental parameter ranges. Then inequality (9) can be satisfied for all $p \in \mathcal{W}$ selecting ϵ as the minimum, with respect to p in $\mathcal{W}$, of the smallest singular value of the Jacobian matrix of $\tilde{Q}$. Condition (14) corresponds to the intuitive requirement that in any configuration of the plasma, each component of the thermal power can be independently changed by a suitable variation of the magnetic parameters p.

Remark 2: Assumption 1 may be partly relaxed further requiring that inequality (9) be satisfied only at $p = p_0$, where p_0 defines a desired *pre-programmed* value for the plasma parameters. Then there exists a non-empty open set $\mathcal{W}_o$ containing p_0 in which the inverse of the Jacobian of $\tilde{Q}$ is well-defined and the results of Theorem 1 holds for p_δ *sufficiently* small, namely such that $p_0 + p_\delta(t) \in \mathcal{W}_o$ for all $t \geq 0$. See also Section IV for more details.

The results presented in Theorem 1 entail that Problem 1 can be solved while additionally enforcing a desired linear behavior $\ddot{T}_{\rm ref}$ to $\ddot{T}$ provided the inverse of a Jacobian matrix is computed. The latter computation, however, may introduce numerical errors in the control scheme since performing the inversion of a Jacobian matrix is not desirable in the presence of noise or approximate models. Therefore, the following proposition provides, under an additional assumption, an alternative control scheme that solves Problem 1 and that trades robustness with exponential stability.

Assumption 2: For any $T_{\rm ref} > T_{\rm eq}$ there exists p^* such that

$$\rho\tilde{Q}(p^*) = \Lambda(T_{\rm ref} - T_{\rm eq}). \tag{15}$$

Fixing any $T_{\rm ref} > T_{\rm eq}$, Assumption 2 requires the existence of some values for the plasma parameters p such that system (8) has an equilibrium at $T = T_{\rm ref}$. Let now $x_1 \in \mathbb{R}^3$ be defined as above and $\xi_2 = \rho\left(\tilde{Q} - \tilde{Q}^*\right) \in \mathbb{R}^3$, with $\tilde{Q}^* \triangleq \tilde{Q}(p^*)$. Then, the evolution of $x_1(t)$ and $\xi_2(t)$ is described by

$$\dot{x}_1 = -\Lambda x_1 + \xi_2, \tag{16a}$$

$$\dot{\xi}_2 = \rho \frac{\partial \tilde{Q}}{\partial p}(p)\dot{p}_\delta. \tag{16b}$$

Theorem 2: Consider system (16) and suppose that Assumption 1 and Assumption 2 hold. Select

$$\dot{p}_\delta = -\Gamma \left(\frac{\partial \tilde{Q}}{\partial p}(p)\right)^\top \xi_2, \tag{17}$$

with $\Gamma = \Gamma^\top > 0$. Then, the zero equilibrium $(x_1, \xi_2) = (0, 0)$ of system (16)-(17) is globally asymptotically stable, hence (17) provides a solution to Problem 1. □

Note that the measured temperatures T are not employed in the feedback scheme of Theorem 2, rendering the latter scheme simpler to implement than the scheme of Theorem 1. Moreover, To compute the desired parameters deviations p_δ via (17) the knowledge of p^* that satisfies (15) may be avoided since only $Q^* = \Lambda(T_{\rm ref} - T_{eq})/\rho$ is required. However, if the parameters Λ, T_{eq} and ρ are not perfectly known, the control scheme of Theorem 2 will steer the temperatures T towards values that are in general different from T_{ref}. Conversely, the feedback scheme of Theorem 1 and Figure 4, possessing an internal model of the constant reference, will force the temperatures to converge to the desired values T_{ref} even in the presence of uncertainties on the values of Λ, T_{eq} and ρ.

Remark 3: In order to obtain, in practice, an acceptable convergence time of the temperatures T_i, $i = 1, 2, 3$, of the modules to the desired values $T_{\rm ref}$ together with an admissible rate of variation of the references $p(t)$ required by the PCS system, the update law of $p_\delta(t)$, namely $\dot{p}_\delta$ in (17), may be saturated as

$$\dot{p}_\delta = -{\rm sat}_\sigma\left(\Gamma \left(\frac{\partial Q}{\partial p}(p)\right)^\top \xi_2\right), \tag{18}$$

where $\sigma \in \mathbb{R}^3$ is a suitable saturation level and $sat_\sigma(\cdot)$ is the decentralized symmetric saturation function. Since the PCS system is linear and asymptotically stable, then it can be shown by standard two time scale techniques [11] that there exists a small enough $\sigma > 0$ such that the overall closed-loop system is asymptotically stable. This result exploits also the fact that, since the goal of the update law is to reduce the

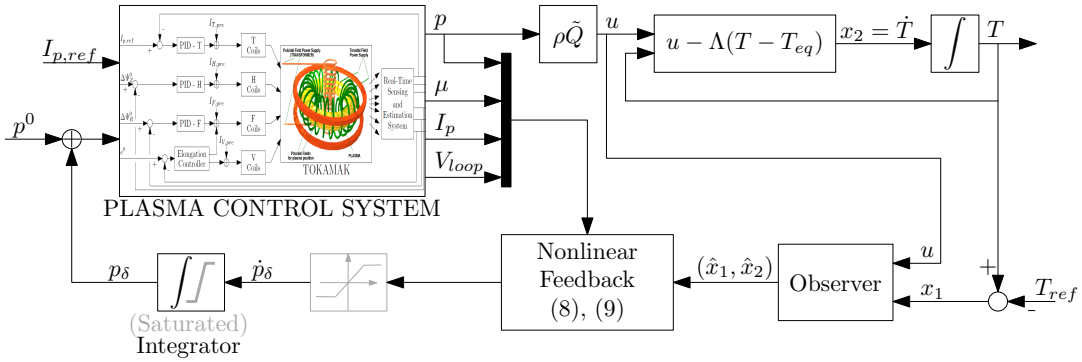

Fig. 4. The feedback scheme of Theorem 1 to control the temperatures of the LLL modules.

thermal power radiating from the plasma, then $\xi_2(t) \geq 0$ for all $t \geq 0$.

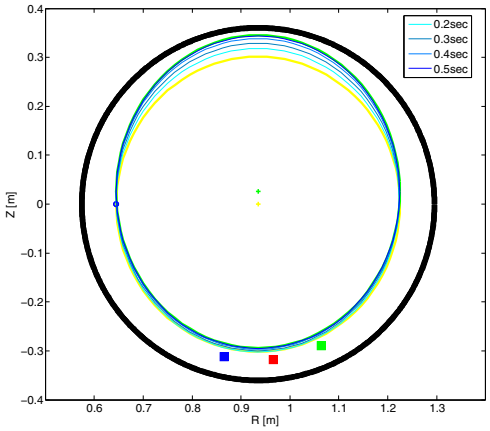

Fig. 5. Initial and final configurations of the plasma inside the vessel without limitations on the plasma parameters p.

IV. Simulation Results

In this section we illustrate the performances of the control law (12) proposed in Theorem 1 by means of numerical simulations. To begin with, we suppose that the plasma configuration $\mu = (r_c, z_c, b)$ may be modified as desired via changes in the plasma parameters $p = (\Delta\Psi_R, \Delta\Psi_Z, e)$. As discussed in Remark 3 a limited rate of update is allowed for the parameters p_δ. The parameters of the simulations are summarized in Table I.

I_p	500 kA	λ_E	$2.05 \cdot 10^{-3}$
V_{loop}	0.3 V	λ_1	1
r_i	0.645 m	λ_2	1
c_R	-0.1	λ_3	1
A_R	0.65	T_{eq}	400 $^\circ C$
γ_R	0.045	T_{ref}	420 $^\circ C$
c_Z	-0.1	$\Delta\Psi_R^0$	0
A_Z	0.65	$\Delta\Psi_Z^0$	0
γ_Z	0.045	e^0	1.04

TABLE I
Simulation parameters.

Figure 5 displays the initial configuration of the plasma (yellow line) inside the vessel (bold line) together with the position of the modules of the Liquid Lithium Limiter (blue, red and green squares). The green line represents the configuration of the plasma once the asymptotic stabilization objective is achieved. In particular, the three temperatures converge to the desired value $T_{ref} = 420^\circ C$, see the dashed lines of Figure 7 that represent the time histories of the temperatures T of the LLL modules. Moreover, displaying different configurations of the plasma at increasing time instants and inspecting the distances represented by the dashed lines in Figure 8 reveals that the Last Closed Magnetic Surface of the plasma is firstly moved *closer* to the three modules. This behavior is due to the fact that the initial temperatures are lower than the desired temperature $T_{\rm ref}$ and it is achieved by increasing the length of the vertical semi-axis b. Then, the surface is moved *away* from the modules by a displacement of its center along the Z-axis.

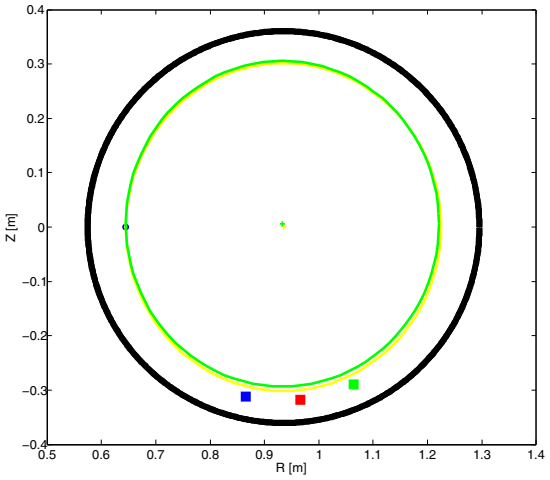

Fig. 6. Initial and final configurations of the plasma inside the vessel in the presence of rate and magnitude limitations on the plasma parameters p.

In practice, the admissible displacements of the plasma configuration, that is the coordinates of the center of the ellipse as well as the length of the vertical semi-axis $\mu = (r_c, z_c, b)$, are extremely limited. Therefore, in order to represent a more realistic scenario, in the last simulation we significantly limit the admissible range of values for the parameters of the ellipse that defines the plasma, by introducing the saturations shown in Figure 4 (see also Remark 3).

In particular we select $[0.5, 0.5, 0.5]$ and $[-0.5, -0.5, -0.5]$ as the maximum and minimum values, respectively, for $\dot{p}_\delta$ and $[0.05, 0.04, 0.02]$ and $[-0.05, -0.04, -0.02]$ as the maximum and minimum values, respectively, for p_δ. With these values, as documented in Figure 6, the large plasma deviations of Figure 5 are avoided. Figure 6 shows the initial and final configurations of the plasma inside the vessel in the presence of rate saturations and limitations on the plasma parameters p.

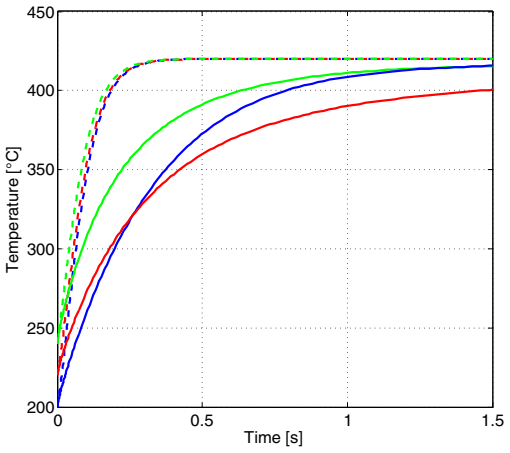

Fig. 7. Time histories of the temperatures T_i, $i = 1, 2, 3$, of the liquid lithium limiter modules with constraints on p (resulting in limitations of the (r_c,z_c)-coordinates and length of the vertical semi-axis) (solid lines) together with the time histories of the temperatures T_i, $i = 1, 2, 3$, of the LLL modules without limitations on p (dashed lines).

It appears evident from the solid curves in Figure 7 that, due to the effect of the saturations, the temperatures T_i, $i = 1, 2, 3$, do not converge to the desired value T_{ref} before the conclusion of the experiment and do not exhibit the desirable linear transient of the dashed curves. Note also that from the solid curves of Figure 8 it appears that the magnitude saturation does not significantly affects the response while the main cause of performance loss is the (rate) saturation imposed on $\dot{p}_\delta$.

V. Conclusions

The temperature control problem of the FTU Liquid Lithium Limiters (LLL) has been considered in this paper. Two alternative techniques have been proposed to tackle the problem. With the first technique, exponential convergence of the temperatures to desired reference values can be guaranteed provided the inverse of a Jacobian matrix is computed. With the second one, inversion may be avoided if exponential convergence is weakened to asymptotic convergence, defining a modified gradient-like algorithm which minimizes the heat absorbed by the modules. Several numerical simulations have been reported to illustrate the performance of the proposed control schemes. Future work includes the development of the controller to be "packaged" as a pluggable module for the FTU Plasma Control System and tested on real experiments.

Acknowledgment

This work was supported by the European Community within the framework of the ENEA/EURATOM Association on Fusion Research. The views and opinions expressed herein do not necessarily reflect those of the European Commission.

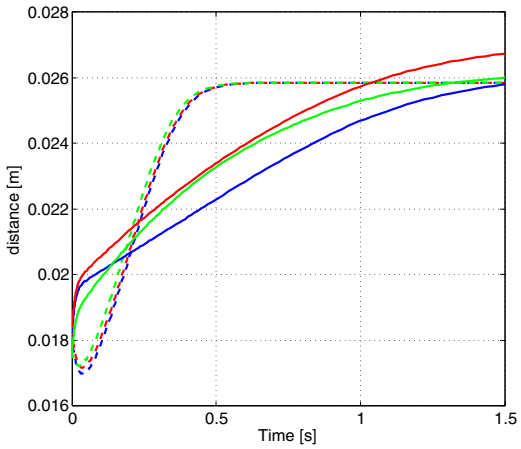

Fig. 8. Time histories of the distances d_i, $i = 1, 2, 3$, of the liquid lithium limiter modules from the Last Closed Magnetic Surface of the plasma with constraints on p (resulting in limitations of the (r_c,z_c)-coordinates and length of the vertical semi-axis) (solid lines) together with the time histories of the distances d_i, $i = 1, 2, 3$, of the LLL modules without limitations on p (dashed lines).

References

[1] G. Mazzitelli, M. Apicella, D. Frigione, G. Maddaluno, M. Marinucci, C. Mazzotta, V. P. Ridolfini, M. Romanelli, G. Szepesi, and O. Tudisco, "FTU results with a liquid lithium limiter," *Nuclear Fusion*, vol. 51, 2011.

[2] L. Zaccarian, L. Boncagni, D. Cascone, C. Centioli, S. Cerino, F. Gravanti, F. Iannone, F. Mecocci, L. Pangione, S. Podda, V. Vitale, and R. Vitelli, "Nonlinear instabilities induced by the F coil power amplifier at FTU: modeling and control," *Fusion Engineering and Design*, vol. 84, no. 7–11, pp. 2015–2019, 2009.

[3] D. Carnevale, A. Astolfi, C. Centioli, S. Podda, V. Vitale, and L. Zaccarian, "A new extremum seeking technique and its application to maximize RF heating on FTU," *Fusion Engineering and Design*, vol. 84, pp. 554–558, 2009.

[4] L. Boncagni, S. Galeani, G. Granucci, G. Varano, V. Vitale, and L. Zaccarian, "Plasma position and elongation regulation at ftu using dynamic input allocation," *Control Systems Technology, IEEE Transactions on*, vol. PP, no. 99, pp. 1–11, 2011.

[5] A. C. Neto, F. Sartori, F. Piccolo, R. Vitelli, G. D. Tommasi, L. Zabeo, A. Barbalace, H. Fernandes, D. F. Valcarcel, and A. J. N. Batista, "MARTe: A multiplatform real-time framework," *IEEE Transactions on Nuclear Science*, vol. 57, no. 2, pp. 479 –486, Apr 2010.

[6] L. Boncagni, Y. Sadeghi, R. Vitelli, C. Centioli, S. Sinibaldi, V. Vitale, L. Zaccarian, and G. Zamborlini, "Progress in the migration towards the real-time framework MARTe at the FTU tokamak," *Fusion Engineering and Design*, 2011.

[7] L. Boncagni, S. Galeani, G. Granucci, G. Varano, V. Vitale, and L. Zaccarian, "Plasma position and elongation regulation at FTU using dynamic input allocation," *IEEE Transactions on Control Systems Technology*, vol. 20, no. 3, pp. 641–651, 2012.

[8] A. Isidori, *Nonlinear control systems*, 3rd ed. Springer, 1995.

[9] V. B. Lazarev, E. A. Azizov, S. V. Mirnov, V. G. Petrov, V. A. Evtikhin, I. E. Lyublinsky, A. V. Vertkov, M. L. Apicella, G. Mazzitelli, and G. Maddaluno, "Litization of ftu tokamak vacuum vessel by using of lithium limiter, proposal for the ftu program on 2003."

[10] E. Sontag, "Remarks on stabilization and input-to-state stability," in *Proc. of the IEEE Conference on Decision and Control*, 1989, pp. 1376–1378.

[11] H. K. Khalil, *Nonlinear systems*, 3rd ed. Prentice Hall, 2002.